

Size and Shape Optimization of Space Trusses Considering Geometrical Imperfection-Sensitivity in Buckling Constraints

Fardad Haghpanah ^{a*}, Hamid Foroughi ^a

^a Department of Civil Engineering, Johns Hopkins University, Maryland, United State.

Received 07 November 2017; Accepted 27 December 2017

Abstract

Optimal design considering buckling of compressive members is an important subject in structural engineering. The strength of compressive members can be compensated by initial geometrical imperfection due to the manufacturing process; therefore, geometrical imperfection can affect the optimal design of structures. In this study, the metaheuristic teaching-learning-based-optimization (TLBO) algorithm is applied to study the geometrical imperfection-sensitivity of members' buckling in the optimal design of space trusses. Three benchmark trusses and a real-life bridge with continuous and discrete design variables are considered, and the results of optimization are compared for different degrees of imperfection, namely 0.001, 0.002, and 0.003. The design variables are the cross-sectional areas, and the objective is to minimize the total weight of the structures under the following constraints: tensile and compressive yielding stress, Euler buckling stress considering imperfection, nodal displacement, and available cross-sectional areas. The results reveal that higher geometrical imperfection degrees significantly change the critical buckling load of compressive members, and consequently, increase the weight of the optimal design. This increase varies from 0.4 to 119% for different degrees of imperfection in the studied trusses.

Keywords: Optimization; Space Trusses; Teaching-Learning-Based-Optimization; Imperfection; Buckling; Metaheuristics.

1. Introduction

Stability of thin-walled members, such as composite plates, shells, and steel cross-sections, is a major concern in the design of lightweight structures [1-4]. For many years, optimal design considering buckling of members under compression was an interesting subject in structural engineering. In 1995, Cheng [5] carried out an optimal solution for truss members with local buckling constraints using the ϵ -relaxed approach. Guo et al. [6] applied a new approach for truss topology optimization with stress and local buckling constraints. Many researchers have proposed different methods to handle the truss optimization problems with buckling constraints [7-10]. New applications of truss elements in robotics to achieve the optimum stiffness-to-weight ratios have brought a new perspective into buckling failure of truss structures. It is well-recognized that the strength of compressive members, specifically thin-walled members such as shells and pipes, is generally influenced by their initial imperfection due to the manufacturing process [11,12]. Initial steps to solve truss optimization problems with local buckling constraints considering sensitivity to geometrical imperfection was carried out by Pedersen and Nielson [13], based on the Danish Standards DS409 using Sequential Linear Programming. In the recent years, different methods have been proposed to study the effects of geometrical imperfection in optimal solution of truss structures. Jalalpour et al. [14] proposed a topology optimization method for the design of trusses with random imperfection using a gradient-based optimizer. Madah and Amir [15] studied local and global buckling of trusses with geometrical imperfection based on geometrically nonlinear beam modeling using the gradient-based Method of

* Corresponding author: fhaghpa1@jhu.edu

 <http://dx.doi.org/10.28991/cej-030960>

➤ This is an open access article under the CC-BY license (<https://creativecommons.org/licenses/by/4.0/>).

© Authors retain all copyrights.

Moving Asymptotes. In this study, geometrical imperfection-sensitivity of members' local buckling constraints in size and shape optimization of small- and large-scale trusses is investigated using a metaheuristic optimization technique.

Application of metaheuristic optimization techniques in engineering and science has become increasingly common. To compare with gradient-based optimization techniques, metaheuristics can be more efficient in solving non-differentiable functions with many local optima [16]. Many metaheuristic methods have been introduced, each with different characteristics, advantages, and relative disadvantages, including: Genetic Algorithm (GA) [17] which is based on the process of natural evolution, Ant Colony Optimization (ACO) [18] which is based on the foraging behaviors of ant colonies, and Particle Swarm Optimization (PSO) [19] which is based on the interactions among a flock of birds. In general, metaheuristics can be divided into two categories: trajectory methods and population-based methods. Teaching-Learning-Based-Optimization (TLBO) is an innovative population-based optimization method developed by Rao et al. [16]. TLBO is inspired from the learning process in schools where the influence of a teacher on learners and the interactions between learners lead to improved performance level of students and a better overall performance of the class. Correspondingly, this method consists of two main phases: the teacher phase and the learner phase. In section 3, the basic methodology of TLBO is explained in detail.

Although gradient-based optimization techniques have specific applications in structural optimization problems (see e.g. [20,21]), metaheuristic optimization methods have a rather extensive application due to the complexity of the search space and design constraints. Many researchers have used these evolutionary techniques for size, shape, and topology optimization of trusses and frames. Rajeev and Krishnamoorthy [22] used GA for size and shape optimization of trusses considering member cross-sections as discrete variables, while Cao [23] took the same approach for framed structures. Fourie and Groenwold [24] used PSO for size and shape optimization of trusses and a torque arm, and Gomes [25] added frequency constraints to the truss optimization using PSO. Kaveh and Zolghadr [26] improved PSO by enhancing its exploration capabilities, and applied the modified PSO for size and shape optimization under frequency constraints. Camp and Bichon [27] used ACO for discrete optimization of space trusses. In recent years, many researchers have used TLBO for design optimization of trusses, frames, and bridges, and they have shown that in comparison with other evolutionary algorithms, TLBO has a competent performance [28-31].

In this paper, the effect of manufacturing geometrical imperfection on buckling constraints in design optimization problems of space trusses is studied. To this end, three benchmark trusses and a real-life bridge are considered for size and shape optimization under the following constraints: tensile and compressive yielding stress, Euler buckling stress considering imperfection, nodal displacement, and available cross-sectional areas. As the optimization algorithm, the teaching-learning-based-optimization technique is used.

2. Truss Optimization Formulation

Size and shape optimization of trusses typically focuses on finding the minimum weight (or cost) of the structure while a set of structural constraints are satisfied. In this study, yielding stress, buckling, nodal displacement, and cross-sectional areas are considered as the strength and serviceability constraints. To this end, the truss optimization problem is formulated as follows:

$$\text{Min}_{A_i} \quad W = \sum_{i=1}^m \rho_i L_i A_i \quad (1)$$

$$\text{s.t.} \quad \sigma_i^l \leq \sigma_i \leq \sigma_i^u \quad (2)$$

$$\sigma_j^b \leq \sigma_j \leq 0 \quad (3)$$

$$\delta_k^l \leq \delta_k \leq \delta_k^u \quad (4)$$

$$A_{\min} \leq A_i \leq A_{\max} \quad (5)$$

$$i \in \{1, 2, \dots, m\}, \quad j \in \{1, 2, \dots, m_c\}, \quad k \in \{1, 2, \dots, n\}$$

Where W is the weight of the truss, m is the number of members, m_c is the number of members in compression, and for each member i , ρ_i is the material unit weight, L_i is the length, A_i is the cross-sectional area, σ_i is the stress, σ_i^l is the stress lower bound corresponding to maximum allowable compressive stress, σ_i^u is the stress upper bound corresponding to maximum allowable tensile stress, σ_j^b is the allowable buckling stress considering imperfection, A_{\min} and A_{\max} are the minimum and maximum allowable cross-sectional areas, respectively, n is the number of nodes, and for each node k , δ_k is the displacement, δ_k^l is the displacement lower bound corresponding to maximum allowable displacement in the negative coordinate, and δ_k^u is the displacement upper bound corresponding to maximum allowable displacement in the positive coordinate. The buckling critical stress considering imperfection in Eq. (3) can be obtained by solving the following equation for σ^b [13]:

$$(\sigma_j^b)^2 - [\sigma_j^y + \sigma_j^{eu}(1 + \eta_j)]\sigma_j^b + \sigma_j^y\sigma_j^{eu} = 0 \tag{6}$$

In which:

$$\sigma_j^{eu} = \frac{\pi^2 E_j I_j}{A_j L_j^2} \tag{7}$$

$$\eta_j = \frac{V_j c_j}{r_j} \tag{8}$$

Where for each compressive member j , σ_j^y is the yield stress, σ_j^{eu} is the Euler buckling stress, E_j is the elastic modulus, I_j is the second moment of area, V_j is the imperfection (i.e. initial deflection at the center of the member), c_j is the distance from the neutral axis to the point of maximum compressive stress, and r_j is the radius of gyration. Radius of gyration can be approximately calculated based on the cross-sectional area as $r = aA^b$ for different available sections. For hollow pipes, $a = 0.4993$ and $b = 0.6777$ [32].

A penalty function is multiplied by the weight of the truss to account for constraint violation. The stress penalty for truss design d , P_d^{str} , is defined as:

$$P_i^{str} = \begin{cases} \left| \frac{\sigma_i - \sigma_i^{l,u}}{\sigma_i^{l,u}} \right| & \text{if } \sigma_i < \sigma_i^l \text{ or } \sigma_i > \sigma_i^u \\ 0 & \text{if } \sigma_i^l \leq \sigma_i \leq \sigma_i^u \end{cases} \tag{9}$$

$$P_d^{str} = \sum_{i=1}^m P_i^{str} \tag{10}$$

The buckling penalty for truss design d , P_d^{bkl} , is defined as:

$$P_j^{bkl} = \begin{cases} \left| \frac{\sigma_j - \sigma_j^{bkl}}{\sigma_j^{bkl}} \right| & \text{if } \sigma_j \leq \sigma_j^{bkl} \leq 0 \\ 0 & \text{if } \sigma_j^{bkl} \leq \sigma_j \leq 0 \end{cases} \tag{11}$$

$$P_d^{bkl} = \sum_{j=1}^{m_s} P_j^{bkl} \tag{12}$$

The displacement penalty for truss design d , P_d^{dis} , in the x , y , and z directions is defined as:

$$P_{k(x,y,z)}^{dis} = \begin{cases} \left| \frac{\delta_{k(x,y,z)} - \delta_k^{l,u}}{\delta_k^{l,u}} \right| & \text{if } \delta_{k(x,y,z)} < \delta_k^l \text{ or } \delta_{k(x,y,z)} > \delta_k^u \\ 0 & \text{if } \delta_k^l \leq \delta_{k(x,y,z)} \leq \delta_k^u \end{cases} \tag{13}$$

$$P_d^{dis} = \sum_{k=1}^n P_{k(x,y,z)}^{dis} \tag{14}$$

The total penalty for truss design d , P_d , is defined as:

$$P_d = (1 + P_d^{str} + P_d^{bkl} + P_d^{dis})^\alpha \tag{15}$$

The value of α is set to 2 as suggested in other studies [31]. Thus, the penalized objective function for truss design d can be obtained as:

$$F_d = W_d P_d \tag{16}$$

3. Teaching-Learning-Based-Optimization

In the TLBO method, the design variables (or the variable vector) are considered as the students in a classroom. The main objective of the algorithm is to improve the performance of each student, and therefore the average performance of the class, in each iteration. This is implemented through interactions between students and the teacher and cooperative interactions between students. The original structure of the TLBO method consists of two phases: the Teacher Phase in which the best student is selected as the teacher (i.e. the best design vector), and the students (i.e. all design vectors) update their knowledge (i.e. their values) to move towards the teacher; and the Learner Phase in which each student finds a classmate, and updates its status based on the classmate's current performance. Below, the detailed steps of the TLBO algorithm is explained.

3.1. Teacher Base

The teacher phase simulates the influence of the teacher on the students in improving their knowledge. To this end, each design variable is regarded as a subject; therefore, each student's current knowledge in all the subjects is represented by a design vector. In truss optimization, the cross-sectional area of each member is a design variable, and a design vector is an array consisting of all the members' cross-sectional areas. In a class with a certain number of students, the best student, which is corresponding to the design vector with minimum design weight, is selected as the teacher. All other design vectors are then updated based on the design variables of the teacher. This teaching activity can be expressed as follows:

$$X_d^{new}(i) = X_d^{old}(i) \pm \Delta(i) \quad (17)$$

$$\Delta(i) = T_F r |M(i) - T(i)| \quad (18)$$

Where for design variable i and design vector d , $X_d^{old}(i)$ is the current value, $X_d^{new}(i)$ is the updated value, $\Delta(i)$ is the difference between the teacher and the class' mean, T_F is the teaching factor, r is a random number uniformly distributed in $[0, 1]$, $M(i)$ is the class' mean, and $T(i)$ is the status of the teacher. In Eq. (17) the sign of $\Delta(i)$ should be selected such that the student's performance moves towards that of the teacher. The value of the teaching factor (T_F) is either 1 or 2, randomly. In this study, a value of $T_F = 2$ is selected, as suggested by Rao et al. [16], to provide a balance between exploitation and exploration aspects of the search domain. The class' mean is generally calculated as:

$$M(i) = \frac{1}{N} \sum_{j=1}^N X_d(i) \quad (19)$$

Where N is the number of students. Camp and Farshchin [31] proposed a weighted mean which improves the performance of TLBO by emphasizing on the highly qualified students:

$$M(i) = \frac{\sum_{d=1}^N \frac{X_d(i)}{F_d}}{\sum_{d=1}^N \frac{1}{F_d}} \quad (20)$$

Where F_d is the penalized objective function for design vector d as in Eq. (16).

3.2. Learner Phase

The learner phase represents the cooperative learning interactions among students. This procedure is executed as follows: (1) randomly select a student p from the class; (2) randomly select a classmate q such that $q \neq p$; (3) evaluate the penalized objective functions F_p and F_q ; and (4) update the state of student p using Eq. (21).

$$X_p^{new}(i) = \begin{cases} X_p^{old}(i) + r [X_p^{old}(i) - X_q(i)] & \text{if } F_p < F_q \\ X_p^{old}(i) + r [X_q(i) - X_p^{old}(i)] & \text{if } F_p \geq F_q \end{cases} \quad (21)$$

Where r is a random number uniformly distributed in $[0, 1]$.

Equation 21 updates the state of student p towards classmate q if the classmate shows a better performance, and away from classmate q if q has a relatively lower performance than student p . Figure 1 illustrates the physics of the learner phase. The student-student interaction iterates for N pairs.

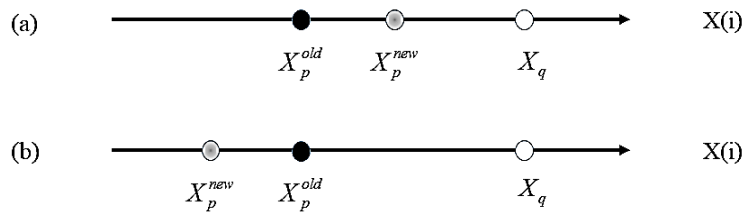


Figure 1. Schematic illustration of the Learner Phase: (a) if student q performs better than student p; (b) if student p performs better than student q

4. Design Examples

Three benchmark truss design problems and a real-life bridge are considered: a 10-bar cantilever truss with ten continuous design variables; a 25-bar transmission tower with eight discrete design variable; a 72-bar multistory truss with sixteen continuous design variables; and a 110-bar truss bridge with continuous design variables for two cases (4 variable groups and 8 variable groups). For all the design problems, a population of 75 students is set, and the TLBO algorithm is implemented for 200 iterations over 100 runs to address possible premature convergence. The results are presented in terms of optimal cross-sectional areas and optimal total weight.

4.1. 10-Bar Truss

Figure 2 illustrates the configuration of the 10-bar truss. The optimal designs for this truss have been obtained using both discrete and continuous cross-sectional areas by means of different optimization techniques [27, 31, 33].

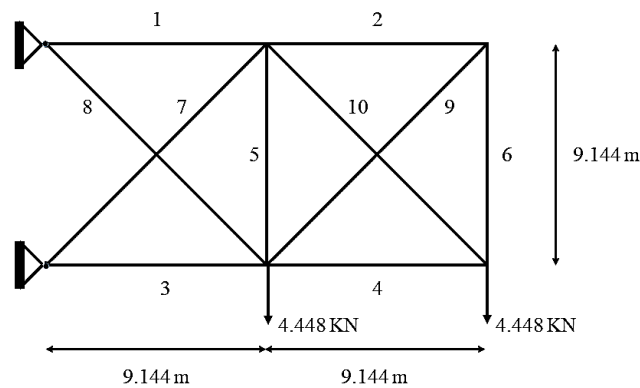


Figure 2. The 10-bar truss

The maximum allowable tensile and compressive stresses in all members are ± 172.369 MPa, the maximum allowable nodal displacement, in both vertical and horizontal directions, is ± 5.08 cm, the material mass density is 2767.990 kg/m³, the material modulus of elasticity is 68947.573 MPa, and the members' cross-sectional area could vary from 0.645 cm² to 225.806 cm².

Table 1 lists the results for different buckling constraints. The optimal weight without the buckling constraints corresponds to results of other studies, specifically to that of Camp and Farshchin [31] which achieved a minimum weight of 2295.6574 kg using TLBO. However, considering Euler buckling with 0, 0.001, 0.002, and 0.003 imperfection, the optimal weight increases by 0.4, 0.6, 0.8, and 1%, respectively. Figure 3 shows the results of a typical convergence history for the 10-bar truss optimization problem.

Table 1. Results for the 10-bar truss

Variables	Cross-sectional areas (cm ²)					
	Camp and Farshchin[31]	Without buckling	With Euler buckling	With 0.001 imperfection	With 0.002 imperfection	With 0.003 imperfection
A ₁	197.8602	196.9164	194.1093	191.3996	188.7816	186.3841
A ₂	0.6452	0.6452	0.6452	0.6452	0.6452	0.6452
A ₃	149.4087	149.6745	152.1810	150.7397	149.3649	148.1287
A ₄	98.2101	98.2146	92.7708	94.9637	97.5837	100.1508
A ₅	0.6452	0.6452	0.6452	0.6452	0.6452	0.6452
A ₆	3.4974	3.5568	0.6452	0.6452	0.6452	0.6452
A ₇	135.6481	135.7088	144.7591	148.6487	152.4668	156.2197
A ₈	48.1638	48.1096	55.7341	56.1773	56.6199	57.0354
A ₉	0.6452	0.6452	0.6452	0.6452	0.6452	0.6452
A ₁₀	138.4900	138.9017	131.1984	129.1010	127.0456	125.1856
Weight (kg)	2295.6574	2295.6032	2305.8023	2308.8493	2313.2686	2318.8336

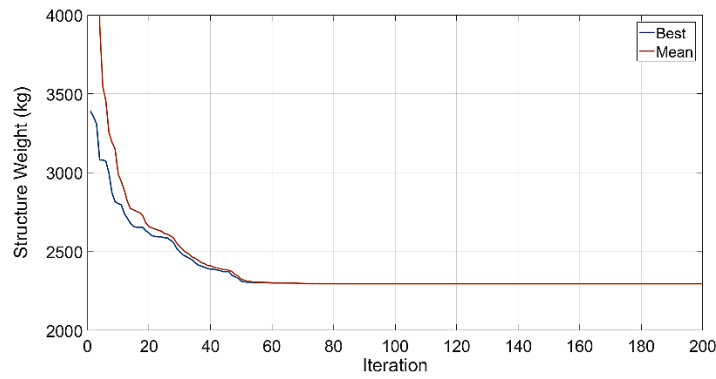


Figure 3. Convergence history for the 10-bar truss problem

The increase in the optimal weight is mostly due to the increase in the cross-sectional areas of elements 7 and 8. Comparing buckling with 0.003 imperfection to the case without buckling constraints, the cross-sectional areas of elements 7 and 8 are increased by 15 and 19%, respectively. Figure 4 illustrates the graphical results for these two design cases. As the optimal weight considering 0.003 imperfection in buckling is only 1% larger than that without the buckling constraints, the final designs do not show significant differences.

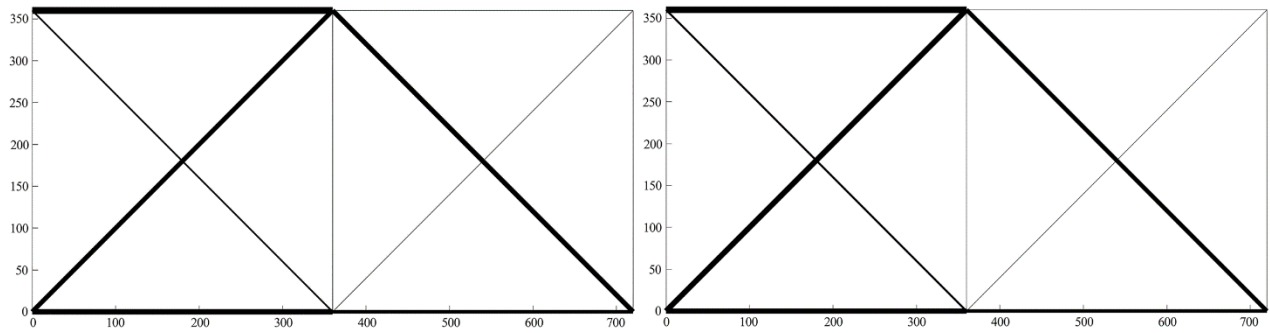


Figure 4. Optimal design of the 10-bar truss: left - without buckling constraints; right - with buckling constraints considering 0.003 imperfection

4.2. 25-Bar Truss

Figure 5 illustrates the configuration of the 25-bar truss. The optimal designs for this truss have been obtained using both discrete and continuous cross-sectional areas by means of different optimization techniques [22,23,27,31].

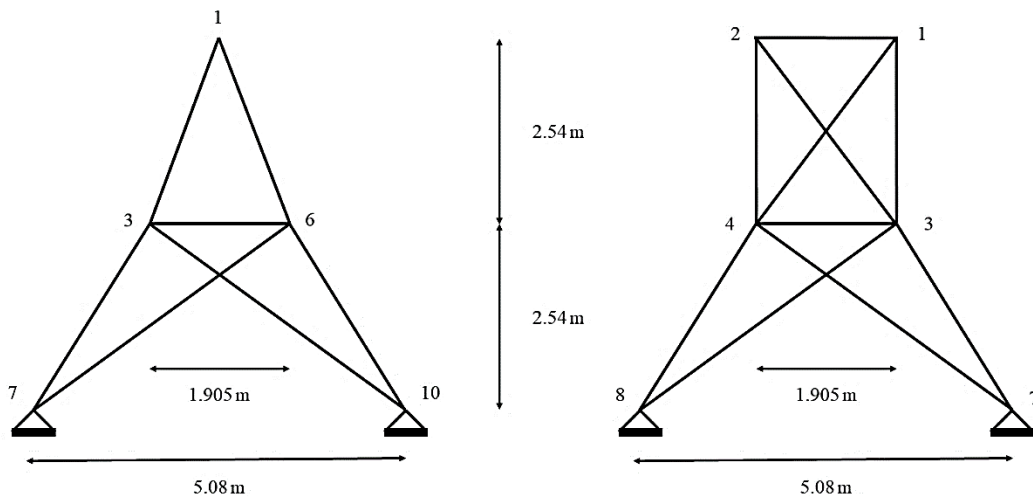


Figure 5. The 25-bar truss: left - front view with dimensions and node numbers, right - side view with dimensions and node numbers

The applied load on the structure is listed in Table 2. The maximum allowable tensile and compressive stresses in all members are ± 275.790 MPa, the maximum allowable nodal displacement, in all directions, is 8.89 mm, the material mass density is 2767.990 kg/m³, the material modulus of elasticity is 68947.573 MPa, and the members' cross-sectional area could vary from 0.645 cm² to 21.935 cm² with increments of 0.645 cm².

Table 2. Single load cases for the 25-bar truss

Node	F _x (KN)	F _y (KN)	F _z (KN)
1	4.448	- 44.482	- 44.482
2	0	- 44.482	- 44.482
3	2.224	0	0
6	2.669	0	0

Table 3 lists the results for different buckling constraints. The optimal weight without the buckling constraint corresponds to results of other studies, specifically to that of Camp and Farshchin [31] who used TLBO and achieved a minimum weight of 219.9243 kg. However, considering Euler buckling with 0, 0.001, 0.002, and 0.003 imperfection, the optimal weight increases by 49, 50, 52, and 53%, respectively. Figure 6 shows the results of a typical convergence history for the 25-bar truss optimization problem.

Table 3. Results for the 25-bar truss

Variables		Cross-sectional areas (cm ²)					
Element group	Members	Camp and Farshchin[31]	Without buckling	With Euler buckling	With 0.001 imperfection	With 0.002 imperfection	With 0.003 imperfection
1	1	0.6452	0.6452	0.6452	1.2903	2.5806	0.6452
2	2-5	1.9355	2.5806	12.9032	12.9032	13.5484	12.9032
3	6-9	21.9354	21.9354	14.8387	14.8387	14.8387	15.4838
4	10,11	0.6452	0.6452	0.6452	0.6452	0.6452	0.6452
5	12,13	13.5484	14.1935	3.2258	3.2258	3.2258	3.2258
6	14-17	6.4516	6.4516	14.1935	14.1935	14.1935	14.1935
7	18-21	3.2258	2.5806	17.4193	17.4193	17.4193	18.0645
8	22-25	21.9354	21.9354	18.7096	19.3548	19.3548	19.3548
Weight (kg)		219.9243	219.6915	327.6196	330.3814	333.4297	335.2656

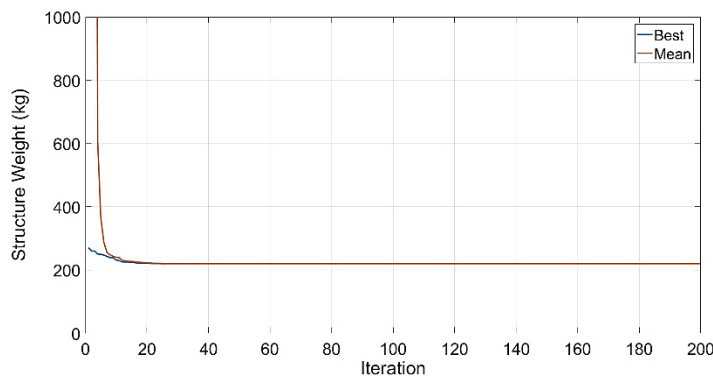


Figure 6. Convergence history for the 25-bar truss problem

The increase in the optimal weight is mostly due to the increase in the cross-sectional areas of element groups 2, 6, and 7. Comparing buckling with 0.003 imperfection to the case without buckling constraints, the cross-sectional areas of element groups 2, 6, and 7 are increased by 400, 120, and 600%, respectively. Figures 7 and 8 illustrate the graphical results for these two design cases.

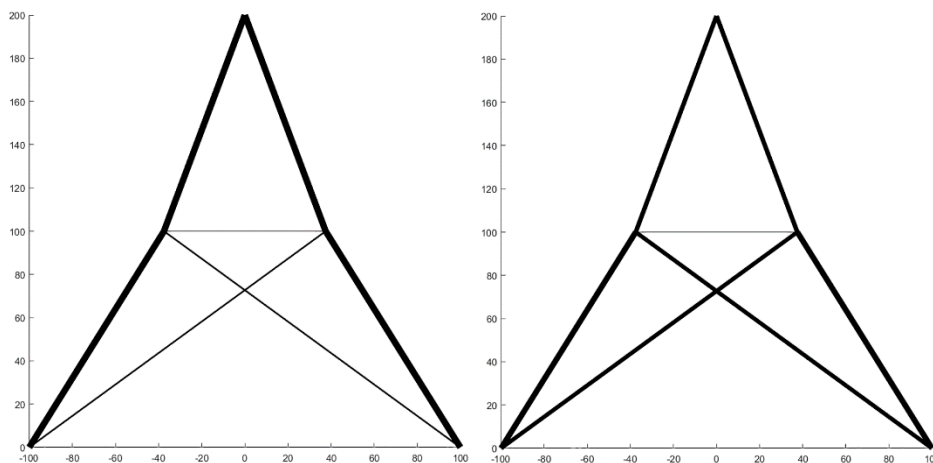


Figure 7. Front view of the optimal design of the 25-bar truss: left - without buckling constraints; right - with buckling constraints considering 0.003 imperfection

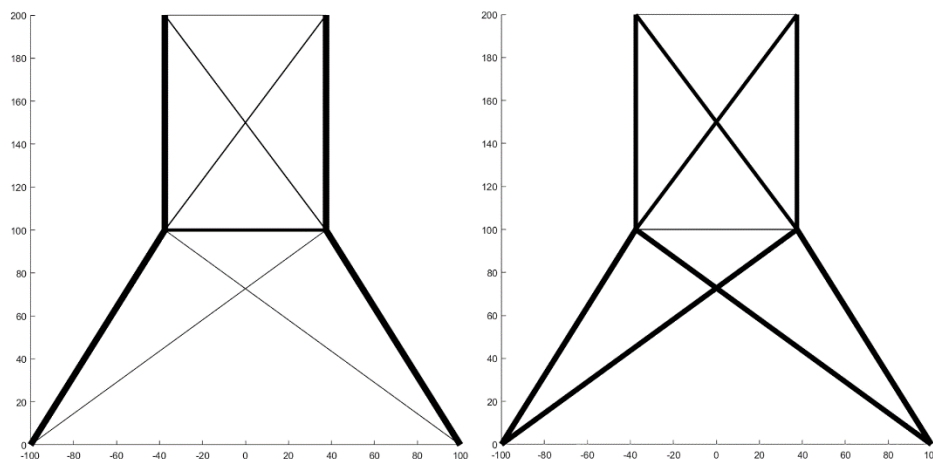


Figure 8. Side view of the optimal design of the 25-bar truss: left - without buckling constraints; right - with buckling constraints considering 0.003 imperfection

4.3. 72-Bar Truss

Figure 9 illustrates the configuration of the 72-bar truss. The optimal design for this truss has been obtained using continuous cross-sectional areas by means of different optimization techniques [23,27,31].

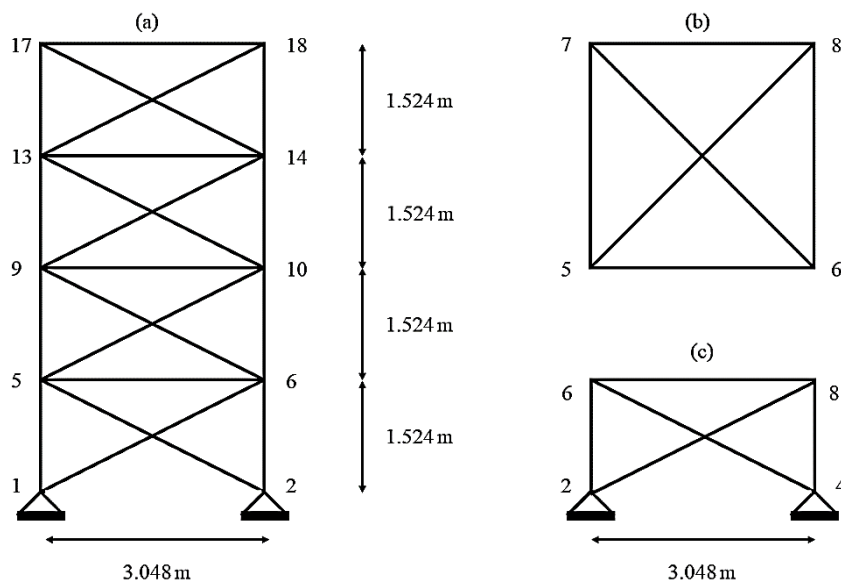


Figure 9. The 72-bar truss: (a) front view with dimensions and node numbering pattern, (b) top view of the first story with dimensions and node numbers, (c) side view of the first story with dimensions and node numbers.

Table 4 shows two load cases applied independently on the structure. The maximum allowable tensile and compressive stresses in all members are ± 172.369 MPa, the maximum allowable nodal displacement, in all directions, is 6.35 mm, the material mass density is 2767.990 kg/m³, the material modulus of elasticity is 68947.573 MPa, and the members' cross-sectional area could vary from 0.645 cm² to 19.355 cm².

Table 4. Independent load cases for the 72-bar truss

Case	Node	F _x (KN)	F _y (KN)	F _z (KN)
1	17	0	0	-22.241
	18	0	0	-22.241
	19	0	0	-22.241
	20	0	0	-22.241
2	17	22.241	22.241	-22.241

Table 5 lists the results for different buckling constraints. The optimal weight without the buckling constraint corresponds to results of other studies, specifically to that of Camp and Farshchin [31] who used TLBO and achieved a minimum weight of 172.2011 kg. However, considering Euler buckling with 0, 0.001, 0.002, and 0.003 imperfection, the optimal weight increases by 112, 113, 116, and 119%, respectively. Figure 10 shows the results of a typical convergence history for the 72-bar truss optimization problem.

Table 5. Results for the 72-bar truss

Variables		Cross-sectional areas (cm ²)					
Element group	Members	Camp and Farshchin[31]	Without buckling	With Euler buckling	With 0.001 imperfection	With 0.002 imperfection	With 0.003 imperfection
1	1-4	12.1335	11.5877	19.3509	12.6484	18.9474	7.1168
2	5-12	3.3174	3.2761	6.5935	6.9387	6.9454	7.5593
3	13-16	0.6452	0.6452	3.2458	2.1174	1.0280	2.3452
4	17,18	0.6452	0.6458	1.1013	5.6839	0.6736	4.1761
5	19-22	8.2006	8.0471	7.1613	6.9381	7.6854	7.6110
6	23-30	3.3232	3.2858	6.9387	6.9284	7.2666	7.1826
7	31-34	0.6452	0.6458	2.5245	2.1581	2.0866	1.8910
8	35,36	0.6452	0.6452	2.7103	1.5329	2.6906	3.0619
9	37-40	3.4303	3.2664	5.5974	5.7426	6.3448	6.0374
10	41-48	3.3123	3.3258	6.5290	6.7310	7.1876	8.1348
11	49-52	0.6452	0.6452	0.6942	0.6645	0.9570	0.8452
12	53,54	0.6452	0.6452	1.9768	3.9981	2.1636	4.2161
13	55-58	1.0097	3.0245	5.8310	6.7142	10.5936	6.3897
14	59-66	3.5026	3.4916	9.2103	8.3322	8.4466	8.6742
15	67-70	2.6329	2.4103	5.9761	8.1600	6.4549	7.6277
16	71,72	3.6987	3.2774	10.0697	9.2355	9.8417	9.4303
Weight (kg)		172.2011	171.8205	364.7387	365.3958	370.9519	376.6399

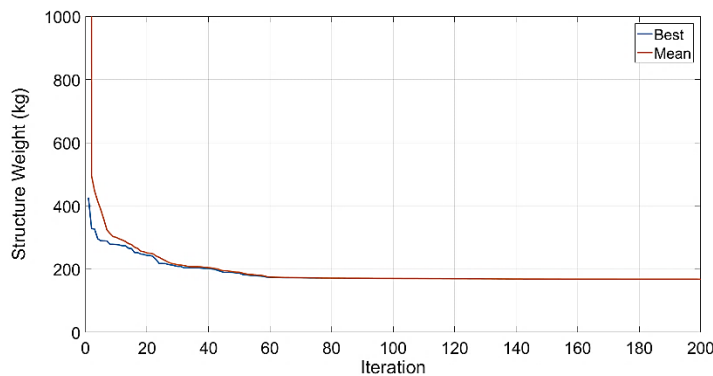


Figure 10. Convergence history for the 72-bar truss problem

The increase in the optimal weight is due to the increase in the cross-sectional areas of all element groups, specifically, groups 4, 8, and 12. Comparing buckling with 0.003 imperfection to the case without buckling constraints, the cross-sectional areas of element groups 4, 8, and 12 are increased by 547, 375, and 554%, respectively. Figure 11 illustrates the graphical results for these two design cases. As the optimal weight considering 0.003 imperfection in buckling is 119% larger than that without the buckling constraints, the final designs show significant differences.

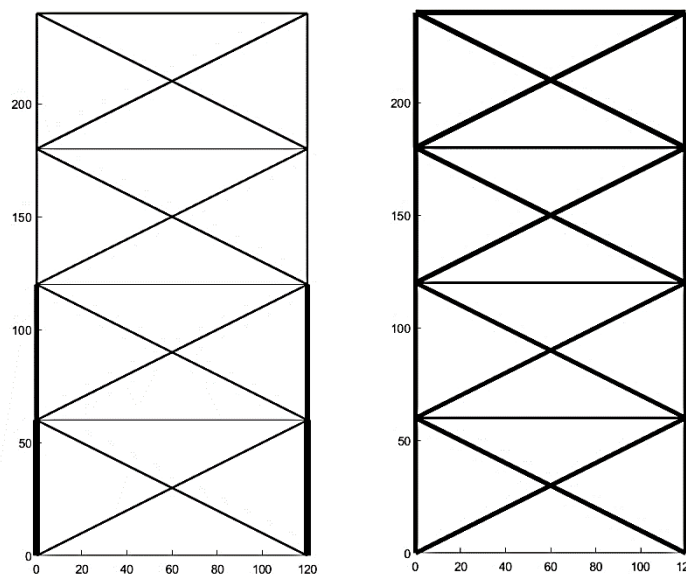


Figure 11. Optimal design of the 72-bar truss: left - without buckling constraints; right - with buckling constraints considering 0.003 imperfection

4.4. The West End Bridge

The West End is a steel tied-arch bridge which passes over the Ohio River in Pittsburgh, Pennsylvania. Built in 1932, the West End Bridge is a braced trussed bridge with pre-stressed hangers between the twin arches and the bottom chords. The engineering and aesthetic qualities of the main span (237 m) made the bridge to be recorded in the US National Register of Historic Places in 1979 [34]. Figure 12 shows the side view of the bridge. The optimal design for this bridge under dead and live loads has been obtained by Makiabadi et al. [29] considering continuous cross-sectional areas and buckling load according to AISC ASD using TLBO. Although Makiabadi et al. considered buckling as a constraint, the effect of imperfection on structural stability is not addressed.



Figure 12. The West End Bridge (source: <http://riverlifepgh.org/riverfront-guide/>)

The total dead and live load on the bridge is 140.539 KN/m, the maximum allowable tensile and compressive stresses in all members are ± 275.790 MPa, the maximum allowable nodal displacement, in all directions, is 29.56 cm, the material mass density is 7929.139 kg/m³, the material modulus of elasticity is 201.097 GPa, and the minimum value of members' cross-sectional area is 139.355 cm². Figure 13 depicts the configuration of the West End truss bridge.

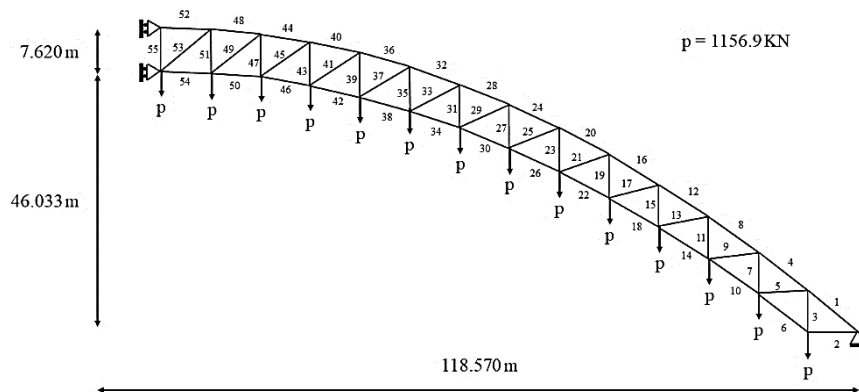


Figure 13. Mid-span dimensions and configuration of the West End Bridge

The members are grouped into 4 and 8 groups for case I and case II, respectively. The member groups are shown in Table 6.

Table 6. Element groups for case I and II

Element groups	Member numbers	
	Case I	Case II
1	2,5,9,13,17,21,25,29,33,37,41,45,49,53	25,29,33,37,41,45,49,53
2	1,4,8,12,16,20,24,28,32,36,40,44,48,52	24,28,32,36,40,44,48,52
3	3,7,11,15,19,23,27,31,35,39,43,47,51,55	27,31,35,39,43,47,51,55
4	6,10,14,18,22,26,30,34,38,42,46,50,54	26,30,34,38,42,46,50,54
5		2,5,9,13,17,21
6		1,4,8,12,16,20
7		3,7,11,15,19,23
8		6,10,14,18,22

Tables 7 and 8 list the results for different buckling constraints for case I and case II, respectively. The optimal weight considering the AISC ASD buckling load is obtained previously by Makiabadi et al. [29] using TLBO to be 250.0423 Ton for case I and 229.5349 Ton for case II. Comparing the optimal weight without buckling constraints with those considering Euler buckling with 0, 0.001, 0.002, and 0.003 imperfection, the optimal weight increases by 10, 22, 32,

and 41%, respectively, for case I, and 7, 20, 30, and 39%, respectively, for case II. Comparison of the results with [29], where the AISC ASD buckling load was used for buckling constraints, reveals that considering 0.003 imperfection, the optimal weight is 6% larger for case I and 5% larger for case II. This implies that the AISC ASD buckling load may underestimate buckling loads of members with 0.003 or larger imperfection. Figure 14 shows the results of a typical convergence history for the West End Bridge optimization problem.

Table 7. Results for the West End Bridge (case I)

Variables	Cross-sectional areas (cm ²)					
	With AISC-ASD buckling [29]	Without buckling	With Euler buckling	With 0.001 imperfection	With 0.002 imperfection	With 0.003 imperfection
A ₁	185.2858	139.3546	152.0823	165.9248	177.9093	189.0577
A ₂	1455.8928	1406.5520	1406.5520	1556.5904	1678.9437	1786.4326
A ₃	139.3546	139.3546	139.3546	139.3546	139.3546	139.3546
A ₄	434.4796	139.3546	313.4549	378.4870	425.0314	465.2584
Weight (Ton)	250.0423	189.1140	207.3344	231.0034	249.7523	266.2179

Table 8. Results for the West End Bridge (case II)

Variables	Cross-sectional areas (cm ²)					
	With AISC-ASD buckling [29]	Without buckling	With Euler buckling	With 0.001 imperfection	With 0.002 imperfection	With 0.003 imperfection
A ₁	174.4255	170.6629	354.4251	464.7010	528.8970	579.9008
A ₂	139.4103	139.3546	139.6333	141.7700	141.1197	139.3546
A ₃	1142.0942	1406.6449	1408.0385	1556.5904	1679.7799	1786.5255
A ₄	207.0251	139.3546	169.7339	194.0745	210.1467	225.1970
A ₅	552.2807	178.8384	356.0044	488.5771	559.1834	614.4607
A ₆	139.3546	139.5404	139.3546	139.3546	142.3275	139.3546
A ₇	1702.0394	1060.9527	926.2433	982.3567	1060.7669	1127.3784
A ₈	465.0447	139.3546	139.3546	139.4475	139.3546	139.3546
Weight (Ton)	229.5349	173.2873	184.8508	208.1232	226.0310	240.6893

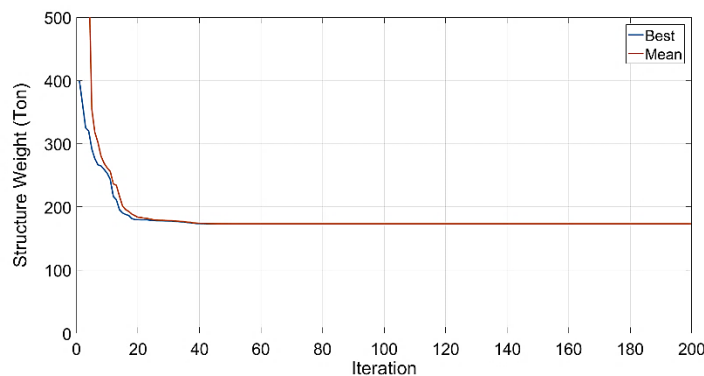


Figure 14. Convergence history for the West End Bridge truss problem (case II)

The increase in the optimal weight is mostly due to the increase in the cross-sectional area of element group 4 for case I and element groups 1 and 5 for case II. Comparing buckling with 0.003 imperfection to the case without buckling constraints, the cross-sectional area of element group 4 in case I is increased by 234%, and the cross-sectional areas of element groups 1 and 5 in case II are increased by 240 and 244%. Figures 15 and 16 illustrate the graphical results for these two design cases.

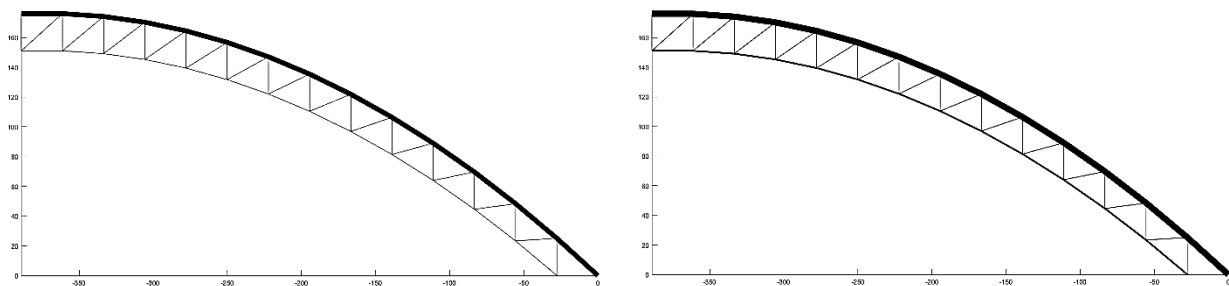


Figure 15: Optimal design of the West End Bridge (case I): left - without buckling constraints; right - with buckling constraints considering 0.003 imperfection

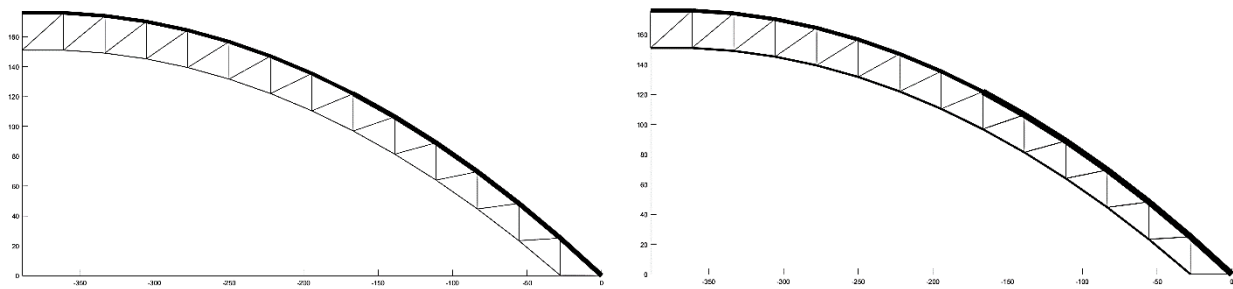


Figure 16: Optimal design of the West End Bridge (case II): left - without buckling constraints; right - with buckling constraints considering 0.003 imperfection

5. Conclusion

In this study, a metaheuristic optimization method is applied for size and shape optimization of space trusses to study the effect of manufacturing geometrical imperfection on members' buckling constraints. The Teaching-Learning-Based-Optimization (TLBO) algorithm is applied to tackle truss optimization problems under different constraints including tensile and compressive yielding stress, buckling stress considering imperfection, nodal displacement, and available cross-sectional areas. Different geometrical imperfection values are considered in the Euler critical buckling loads of compressive members as the local buckling constraints for three benchmark trusses and a real-life bridge. The optimization problems are solved and the results are compared for different imperfection ratios. The optimization results indicate that higher geometrical imperfection degrees make significant changes to the critical buckling load of compressive members, and consequently, increase the weight of the optimal design. This increase in the optimal weight ranges from 0.4% to 119% for the studied structures. Hence, considering geometrical imperfection in the optimal design of truss structures provides solutions that are less sensitive to manufacturing errors and furnish a reliable starting point for design engineers.

6. References

- [1] Iwicki, Piotr, and Marcin Krajewski. "3D buckling analysis of a truss with horizontal braces." *Mechanics and Mechanical Engineering* 17.1 (2013): 49-58.
- [2] Foroughi, Hamid, and Mojtaba Azhari. "Mechanical buckling and free vibration of thick functionally graded plates resting on elastic foundation using the higher order B-spline finite strip method." *Meccanica* 49.4 (2014): 981-993. DOI: 10.1007/s11012-013-9844-2.
- [3] Foroughi, H., H. Askariyeh, and M. Azhari. "Mechanical Buckling of Thick Composite Plates Reinforced with Randomly Oriented, Straight, Single-Walled Carbon Nanotubes Resting on an Elastic Foundation using the Finite Strip Method." *Journal of Nanomechanics and Micromechanics* 3.3 (2013): 49-58. DOI: 10.1061/(ASCE)NM.2153-5477.0000060.
- [4] Gholami Shahrestani, Mojtaba, Mojtaba Azhari, and Hamid Foroughi. "Elastic and inelastic buckling of square and skew FGM plates with cutout resting on elastic foundation using isoparametric spline finite strip method." *Acta Mechanica*. DOI: 10.1007/s00707-017-2082-2.
- [5] Cheng, G. "Some aspects of truss topology optimization." *Structural and Multidisciplinary Optimization* 10.3 (1995): 173-179. DOI: 10.1007/BF01742589.
- [6] Guo, X., G. Cheng, and K. Yamazaki. "A new approach for the solution of singular optima in truss topology optimization with stress and local buckling constraints." *Structural and Multidisciplinary Optimization* 22.5 (2001): 364-373. DOI: 10.1007/s00158-001-0156-0.
- [7] Tugilimana, Alexis, Rajan Filomeno Coelho, and Ashley P. Thrall. "Including global stability in truss layout optimization for the conceptual design of large-scale applications." *Structural and Multidisciplinary Optimization* (2017): 1-20. DOI: 10.1007/s00158-017-1805-2.
- [8] Dunning, Peter D., Evgueni Ovtchinnikov, Jennifer Scott, and H. Alicia Kim. "Level - set topology optimization with many linear buckling constraints using an efficient and robust eigensolver." *International Journal for Numerical Methods in Engineering* 107.12 (2016): 1029-1053. DOI: 10.1002/nme.5203.
- [9] Luo, Quantian, and Liyong Tong. "Elimination of the Effects of Low Density Elements in Topology Optimization of Buckling Structures." *International Journal of Computational Methods* 13.06 (2016): 1650041. DOI: 10.1142/S0219876216500419.
- [10] Cao, Hongyou, Xudong Qian, Zhijun Chen, and Hongping Zhu. "Enhanced particle swarm optimization for size and shape optimization of truss structures." *Engineering Optimization* (2017): 1-18. DOI: 10.1080/0305215X.2016.1273912.

- [11] Foroughi, H., C. D. Moen, A. Myers, M. Tootkaboni, L. Vieira, and B. W. Schafer. "Analysis and design of thin metallic shell structural members-current practice and future research needs." In Proceedings of Annual Stability Conference Structural Stability Research Council, Toronto, Canada. 2014.
- [12] Foroughi, H., Schafer, B. W. "Simulation of conventional cold-formed steel sections formed from advanced high strength steel (AHSS)." arXiv preprint arXiv:1712.08037 (2017).
- [13] Pedersen, Niels L., and Anders K. Nielsen. "Optimization of practical trusses with constraints on eigenfrequencies, displacements, stresses, and buckling." *Structural and Multidisciplinary Optimization* 25.5 (2003): 436-445. DOI: 10.1007/s00158-003-0294-7.
- [14] Jalalpour, Mehdi, Takeru Igusa, and James K. Guest. "Optimal design of trusses with geometric imperfections: Accounting for global instability." *International Journal of Solids and Structures* 48.21 (2011): 3011-3019. DOI: 10.1016/j.ijsolstr.2011.06.020.
- [15] Madah, Hazem, and Oded Amir. "Truss optimization with buckling considerations using geometrically nonlinear beam modeling." *Computers & Structures* 192 (2017): 233-247. DOI: 10.1016/j.compstruc.2017.07.023.
- [16] Rao, Ravipudi V., Vimal J. Savsani, and D. P. Vakharia. "Teaching-learning-based optimization: a novel method for constrained mechanical design optimization problems." *Computer-Aided Design* 43.3 (2011): 303-315. DOI: 10.1016/j.cad.2010.12.015.
- [17] Holland, John Henry. *Adaptation in natural and artificial systems: an introductory analysis with applications to biology, control, and artificial intelligence*. MIT press, 1992.
- [18] Dorigo, Marco. "Optimization, learning and natural algorithms." Ph.D. Thesis, Politecnico di Milano, Italy (1992).
- [19] Kennedy, J. and Eberhart, R. "Particle swarm optimization." Proceedings of IEEE International Conference on Neural Networks IV, pages. Vol. 1000. 1995. DOI: 10.1109/ICNN.1995.488968.
- [20] Behrou R., Guest J. K. "Topology optimization for transient response of structures subjected to dynamic loads." 18th AIAA/ISSMO Multidisciplinary Analysis and Optimization Conference, Denver, CO. 2017. DOI: 10.2514/6.2017-3657.
- [21] Behrou, Reza, Matthew Lawry, and Kurt Maute. "Level set topology optimization of structural problems with interface cohesion." *International Journal for Numerical Methods in Engineering* (2017). DOI: doi.org/10.1002/nme.5540.
- [22] Rajeev, S., and C. S. Krishnamoorthy. "Discrete optimization of structures using genetic algorithms." *Journal of structural engineering* 118.5 (1992): 1233-1250. DOI: 10.1061/(ASCE)0733-9445(1992)118:5(1233).
- [23] Cao, Guozhong. "Optimized design of framed structures using a genetic algorithm." PhD thesis, The University of Memphis, TN (1997).
- [24] Fourie, P. C., and Albert A. Groenwold. "The particle swarm optimization algorithm in size and shape optimization." *Structural and Multidisciplinary Optimization* 23.4 (2002): 259-267. DOI: 10.1007/s00158-002-0188-0.
- [25] Gomes, Herbert Martins. "Truss optimization with dynamic constraints using a particle swarm algorithm." *Expert Systems with Applications* 38.1 (2011): 957-968. DOI: 10.1016/j.eswa.2010.07.086.
- [26] Kaveh, A., and A. Zolghadr. "Democratic PSO for truss layout and size optimization with frequency constraints." *Computers & Structures* 130 (2014): 10-21. DOI: 10.1016/j.compstruc.2013.09.002.
- [27] Camp, Charles V., and Barron J. Bichon. "Design of space trusses using ant colony optimization." *Journal of Structural Engineering* 130.5 (2004): 741-751. DOI: 10.1061/(ASCE)0733-9445(2004)130:5(741).
- [28] Toğan, Vedat, and Ali Mortazavi. "Sizing optimization of skeletal structures using teaching-learning based optimization." *An International Journal of Optimization and Control: Theories & Applications (IJOCTA)* 7.2 (2017): 130-141. DOI: 10.11121/ijocta.01.2017.00309.
- [29] Makiabadi, M. H., A. Baghlani, H. Rahnema, and M. A. Hadianfard. "Optimal design of truss bridges using teaching-learning-based optimization algorithm." *Iran University of Science & Technology* 3.3 (2013): 499-510.
- [30] Toğan, Vedat. "Design of planar steel frames using teaching-learning based optimization." *Engineering Structures* 34 (2012): 225-232. DOI: 10.1016/j.engstruct.2011.08.035.
- [31] Camp, C. V., and M. Farshchin. "Design of space trusses using modified teaching-learning based optimization." *Engineering Structures* 62 (2014): 87-97. DOI: 10.1016/j.engstruct.2014.01.020.
- [32] Saka, M. P. "Optimum design of pin-jointed steel structures with practical applications." *Journal of Structural Engineering* 116.10 (1990): 2599-2620. DOI: 10.1061/(ASCE)0733-9445(1990)116:10(2599).
- [33] Schutte, J. F., and A. A. Groenwold. "Sizing design of truss structures using particle swarms." *Structural and Multidisciplinary Optimization* 25.4 (2003): 261-269. DOI: 10.1007/s00158-003-0316-5.
- [34] Bauman, John. "West End Bridge." *Written Historical and Descriptive Data Historic American Engineering Record*, National Park Service, U.S. Department of the Interior, 1985. From Data Pages, Library of Congress (HAER No. PA-96, available online at: <http://cdn.loc.gov/master/pnp/habshaer/pa/pa1700/pa1732/data/pa1732data.pdf>, accessed Oct. 21, 2017).